JACS
JOURNAL OF THE AMERICAN CHEMICAL SOCIETY
Article
pubs.acs.org/JACS

Ion Intercalation into Two-Dimensional Transition-Metal Carbides: Global Screening for New High-Capacity Battery Materials

Christopher Eames and M. Saiful Islam*

Department of Chemistry, University of Bath, Bath BA2 7AY, United Kingdom

Supporting Information

ABSTRACT: Two-dimensional transition metal carbides (termed MXenes) are a new family of compounds generating considerable interest due to their unique properties and potential applications. Intercalation of ions into MXenes has recently been demonstrated with good electrochemical performance, making them viable electrode materials for rechargeable batteries. Here we have performed global screening of the capacity and voltage for a variety of intercalation ions (Li^+, Na^+, K^+, and Mg^{2+}) into a large number of M_2C-based compounds (M = Sc, Ti, V, Cr, Zr, Nb, Mo, Hf, Ta) with F-, H-, O-, and OH-functionalized surfaces using density functional theory methods. In terms of gravimetric capacity a greater amount of Li^+ or Mg^{2+} can be intercalated into an MXene than Na^+ or K^+, which is related to the size of the intercalating ion. Variation of the surface functional group and transition metal species can significantly affect the voltage and capacity of an MXene, with oxygen termination leading to the highest capacity. The most promising group of M_2C materials in terms of anode voltage and gravimetric capacity (>400 mAh/g) are compounds containing light transition metals (e.g., Sc, Ti, V, and Cr) with nonfunctionalized or O-terminated surfaces. The results presented here provide valuable insights into exploring a rich variety of high-capacity MXenes for potential battery applications.

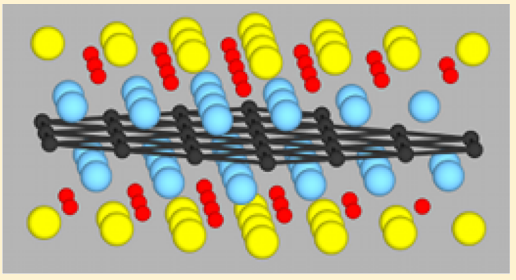

1. INTRODUCTION

Two-dimensional (2D) materials such as graphene are currently a topic of intense interest. A significant recent discovery is the new family of 2D early transition metal carbides,[1,2] which are often termed "MXenes" to indicate their structural similarities with graphene; a range of favorable properties have been investigated for possible applications.[3−14] One such application is energy storage, which is critical to achieving the important goal of clean sustainable energy. It is clear that major advances in electrochemical energy storage for portable electronics, electric vehicles, and electricity grid systems will depend on the discovery and optimization of new high-performance materials. Recently, intercalation of ions onto the functionalized surfaces of MXenes was demonstrated[3−6] with a high rate capability, high storage capacity, and low intercalation voltages, making them promising materials for both supercapacitors and ion intercalation batteries.

MXenes form a 2D layered structure with the general formula $M_{n+1}X_n$ (where M = Sc, Ti, V, Cr, Zr, Nb, Mo, Hf, Ta; X = C, N; and typically n = 1, 2, or 3). The M_2C structure is shown in Figure 1 and comprises a central hexagonal graphene layer capped on both sides by a transition metal layer. Naguib et al.[5] showed that selective etching of the A group from MAX phases (e.g., Ti_2AlC) results in the formation of 2D carbides such as Ti_2C. During synthesis, contact with hydrofluoric acid (HF) leads to functionalization of the MXene surface by O, OH, and a small amount of F.[3−5] For this reason MXenes are often labeled $M_{n+1}X_nT_x$ where T_x denotes the mixture of functional groups that terminate each surface. Numerous compositions have been synthesized,[3−5] and ion intercalation onto the surfaces of Nb_2C, Ti_2C, V_2C, and Ti_3C_2 has been achieved by experiment.[3,5]

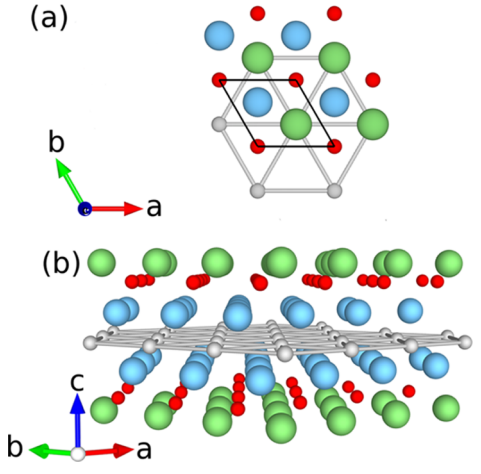

Figure 1. Two-dimensional M_2C structure: (a) view down the c-axis and (b) side view. Key: green, intercalant; red, functional group; blue, transition metal; gray, graphitic C. In the top view the 1x1 unit cell is outlined in black, and for clarity only the first four layers are shown.

Computational modeling[11,15−23] has provided key insights into a number of aspects of MXenes including the atomic and

Received: August 8, 2014
Published: October 13, 2014

   dx.doi.org/10.1021/ja508154e | J. Am. Chem. Soc. 2014, 136, 16270−16276

electronic structure, elastic properties, surface functionalization, and the formation of nanoscrolls from the rolling of the MXene layers. The functional group attachment sites across the series have been identified.[11,18] Tang et al.[17] have also examined the favorable sites for Li insertion into functionalized $Ti_3C_2T_2$ and revealed that the functional group affects both the voltage and the capacity of the system. Crucially, the calculated formation energies of possible MXenes that have not yet been synthesized suggest that many more MXene compositions may be energetically stable.

In the context of energy storage, lithium-ion batteries have helped power the revolution in portable electronics due to their high gravimetric energy density,[24−28] with growing use in electric vehicles. Recently, there has been renewed interest in alternatives to lithium. Sodium[29,30] offers a more abundant, lower cost, and electrochemically comparable option to lithium-based counterparts, but the graphite anode is problematic for Na-ion batteries. Divalent intercalating ions such as Mg^{2+} are also attractive[31,32] since the intercalation of each ion is a two-electron process that effectively doubles the capacity per formula unit. However, magnesium-based batteries have presented formidable obstacles, such as finding compatible electrolytes, which have prevented their use, and the intercalation of divalent ions in typical 3D intercalation compounds is poorly understood. For the 2D MXenes, intercalation occurs directly from solution, resulting in a higher rate capability than that observed for typical 3D intercalation hosts; intercalation of Mg^{2+} in MXenes was also recently demonstrated.[3]

A key property of an energy storage material is the gravimetric capacity. MXenes have been reported with reversible capacities of 170 and 260 mAh/g for Nb_2C- and V_2C-based electrodes, respectively, in Li-ion battery cells.[33] These values are not as high as that for the dominant anode material, graphite,[24] at around 350 mAh/g. The capacity thus needs to be improved. However, an extensive range of MXene compositions has not been fully explored. Computational methods based on atomistic potentials and density functional theory (DFT) now play a vital role in characterizing and predicting the properties of new promising materials.[28]

In this work we use DFT methods to perform a global search across the M_2Xene family via a combinatorial screening process of over 300 compounds to identify those with a high intercalation capacity and favorable voltage. In particular, common monovalent (Li^+, Na^+, K^+) and divalent (Mg^{2+}) intercalating ions have been intercalated into M_2C-based compounds (M = Sc, Ti, V, Cr, Zr, Nb, Mo, Hf, Ta) capped with F, H, O, and OH surface functional groups. The present study plays a predictive role in suggesting promising new battery materials for future synthesis and electrochemical work to add to the limited M_2C phases that have been tested so far.

2. METHODOLOGY

2.1. DFT and Structure Simulation. Since our study is based on well-established DFT techniques that have been applied to other battery materials[28,34−40] and high-throughput searches,[41−45] a brief overview is presented here. Relaxed atomic structures and total energies were computed using the plane-wave DFT based code VASP.[46] Core electrons were treated using PAW pseudopotentials,[47] and electron correlation was treated using the Perdew−Burke−Ernzerhof (PBE) generalized gradient approximation.[48] Xie and Kent have shown that for MXenes higher order treatment of correlation effects is unnecessary.[18] A 600 eV cutoff energy for the plane wave basis set together with a 12×12×1 reciprocal space sampling mesh was found to adequately converge the stress for cell shape relaxation. Atomic positions and in-plane lattice parameters were relaxed until the stress was converged to better than 0.05 GPa and the atomic forces were below 0.005 eV/Å. Fully delaminated MXenes are used since these offer a higher rate capability, and this was achieved by fixing the *c* axis of all cells at 50 Å. We have focused on the M_2X phases which have the lowest mass per formula unit and hence the highest gravimetric capacity. The starting point for all structural optimizations was the comprehensive set of calculated lattice parameters of Ti_2C reported by Xie and Kent.[18] Functional groups were added in the three-fold hollow site above the three neighboring C atoms in the graphitic central layer. Several studies have shown that for the majority of MXenes this is the most favorable location.[11,17,18,21] Two Li, Na, K, or Mg atoms were inserted per formula unit at the surface in the site directly above the central C atoms after Tang et al.[17] The intercalated geometry is a single monolayer on each surface of the MXene slab in a 1×1 unit cell (see Figure 2). We emphasize that our aim is global screening; the finer details of the most promising compounds are intended for future work.

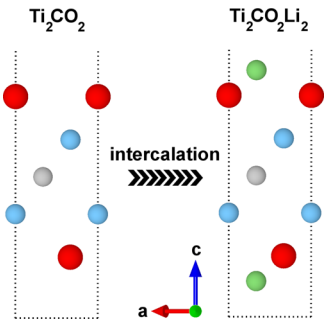

Figure 2. Schematic of an intercalation reaction using lithium insertion in Ti_2CO_2 as an example. Key: green, lithium; red, oxygen; blue, titanium; gray, graphitic C. The unit cell is outlined and extends to 50 Å along the *c* axis.

A complete set of structural parameters for all compounds is contained in the Supporting Information (SI). There is very limited experimental data on the in-plane lattice parameter (**a**) of MXenes for direct comparison since the nanocrystalline nature of the material makes this difficult to obtain. So far, in-plane lattice parameters have only been reported via pair distribution function analysis for pristine and intercalated $Ti_3C_2T_x$, and no data are reported for the M_2X phases.[49] We note, however, that our calculated data are in excellent agreement with other computational studies, giving us confidence in the structural reproduction.

One noteworthy structural change that we observe on intercalation is a change in the in-plane lattice parameter. In general, the in-plane lattice parameter increases upon intercalation. A clear relation between this expansion and the ionic radius of the intercalating ion is present. For example, after intercalation the Ti_2C lattice parameter of 3.082 Å increases to 3.117 Å (+1.1%) for Mg^{2+}, 3.115 Å (+1.0%) for Li^+, 3.205 Å (+4.0%) for Na^+, and 3.334 Å (+8.5%) for K^+, and the respective ionic radii are 72 pm for Mg^{2+}, 76 pm for Li^+, 102 pm for Na^+, and 138 pm for K^+. The implication is that the larger ions experience greater lateral electrostatic repulsion when intercalated, leading to larger in-plane lattice constants. A small number of functionalized MXenes undergo a slight contraction of the **a** lattice parameter on intercalation such as $Li_2Ti_2CO_2$ where the lattice parameter reduces from 3.032 to 3.018 Å (−0.5%), which may be caused by reduced lateral interactions between the surface functional groups due to changes in charge distribution after intercalation.

2.2. Capacity and Voltage. To determine which intercalating species offers the most favorable energy storage properties we have computed the theoretical capacity and cell voltage for intercalation of a full monolayer coverage on each MXene surface, which corresponds to two Li^+, Na^+, K^+, or Mg^{2+} per formula unit (Figure 2). The theoretical gravimetric capacity, *Q*, is determined from

dx.doi.org/10.1021/ja508154e | J. Am. Chem. Soc. 2014, 136, 16270−16276

$$Q = \frac{nF}{M_f} \quad (1)$$

where n is the number of electrons transferred per formula unit (in this case 2 for Li^+, Na^+, and K^+, and 4 for Mg^{2+}), F is the Faraday constant, and M_f is the mass of the formula unit. The current is assumed to be at a 1 C rate (full charge/discharge in 1 h). For the following general intercalation reaction (using Li as the example intercalating ion),

$$M_2CT_x + 2Li \rightarrow M_2CT_xLi_2 \quad (2)$$

the voltage is computed using a well-established approach[50] according to the formula

$$V = \frac{-[E(M_2CT_xLi_2) - E(M_2CT_x) - 2\mu(Li)]}{2} \quad (3)$$

where $E(M_2CT_x)$ is the total energy of the MXene compound, $E(M_2CT_xLi_2)$ is the total energy of the MXene after intercalation of two atoms per formula unit, and $\mu(Li)$ is the chemical potential of the intercalating species. Equation 3 is defined such that a positive voltage indicates energetically favorable intercalation. Such computational methods have been applied successfully to a range of Li- and Na-ion battery materials.[28,34−43]

3. RESULTS AND DISCUSSION

3.1. Global Screening of Voltage and Capacity. In recent experimental work, the voltage of a few MXenes is observed to change during intercalation, which is behavior typically associated with the formation of a solid solution. For example, at the start of charge, Nb_2CT_x has a voltage of around 2.4 V, which falls to about 0.4 V after intercalation at 100 mAh/g and to 0 V at 250 mAh/g; this shows a nonlinear variation with two-thirds of the capacity removed below 1 V.[33] These electrochemical experiments indicate that a voltage window is obtained (rather than a specific voltage), and it is therefore not valid to compare average voltages computed by DFT with the voltage measured at 50% of the reversible capacity. It is for this reason that we have compared our computed average voltages with observed voltage windows.

In first assessing the validity of our DFT approach it is found that the trend in experimental voltages for Li-ion cells is reproduced by our calculations. Nb_2C is observed to intercalate two-thirds of its capacity below 1 V,[33] and our calculations predict an average voltage of 0.89 V; for V_2C an average voltage of 1.43 V[33] is calculated, and from experiment two-thirds of the capacity is above 1.5 V; Ti_2C intercalates 50% of its capacity above 1 V, and the calculated average voltage is 1.22 V.[5] These calculated values are for oxygen termination, whereas in the electrochemical work a variety of surface functional groups are possible. Nevertheless, the general good agreement between the calculated and experimental voltage trends provides further support to the screening approach used here. We note that recent DFT work of Xie et al.[51] on lithium intercalation into MXenes complements the results of our study; they consider three M_2C-based compounds at slightly different stoichiometries containing less oxygen than the compositions here. Although our focus has been on the carbides, it is worth commenting that we have also performed similar calculations for a wide range of M_2N based compounds; the resulting data are presented as SI and in general indicate slightly lower capacities than the M_2C-based compounds.

In addition to voltages we also analyzed how the maximum theoretical capacities compare to practical measured capacities that are currently available. The electrochemical properties of three M_2C phases that have so far been reported[5,33] to successfully cycle Li^+ are listed in Table 1. As noted, experiments indicate that MXenes are terminated mostly by oxygen, and so we have used our data for oxygen terminated systems for comparison. The data indicate that, at most, 78% of the theoretical capacity is reached. A number of factors are known to contribute including particle size, in which smaller particles offer a higher reversible capacity due to greater penetration between the MXene layers during cycling (e.g., in V_2C, milled samples show a reversible capacity of 288 mAh/g versus 210 mAh/g in unmilled samples[33]); solid electrolyte interphase (SEI) formation; solvation effects when intercalation occurs from solution; and the possibility of intercalation of solvated ions onto the MXene surface.[51]

Table 1. Current Experimental Data on Reversible Capacities for Li/MXenes and Their Maximum Theoretical Capacity (Based on Monolayer Intercalation and Oxygen Termination)

MXene	experimental reversible capacity (mAh/g)[5,33]	theoretical capacity (mAh/g)
Nb_2CO_2	170	250
V_2CO_2	260	335
Ti_2CO_2	110	350

The data in Table 1 show that the theoretical capacity is a useful guide to the practical capacity and suggest correctly that V_2CO_2 should have a higher capacity than Nb_2CO_2. We note that the earlier data reported for Ti_2CT_x represent only 30% of its theoretical capacity, whereas the more recent data for Nb_2CT_x and V_2CT_x achieve 72% and 87%, respectively, of the theoretical capacity. It is of interest whether this is due to fundamental differences in electronic structure and/or solid solution behavior or simply an improvement in the sample preparation procedure.

We next used DFT methods to perform a global search across the M_2Xene family via a combinatorial screening process encompassing more than 300 compounds to identify those with a high intercalation capacity and favorable voltage. The computed results for all M_2C phases are presented in Figure 3. The results reveal two main features. First, it is clear that a wide range of electrochemical properties are present in this family of compounds and that these are sensitive to the intercalating species. Second, a number of Li^+ and Mg^{2+}

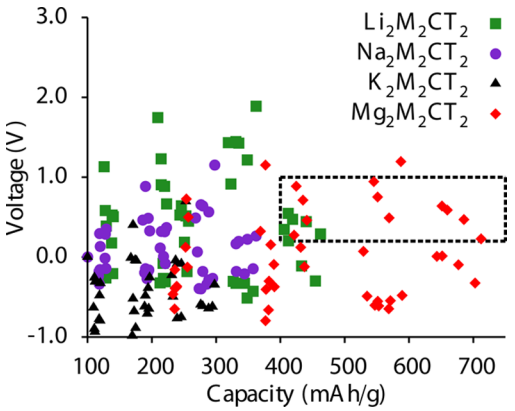

Figure 3. Cell voltage and theoretical gravimetric capacity for intercalation of two ions of Li^+, Na^+, K^+, or Mg^{2+} per formula unit into M_2CT_2 MXenes (where M refers to the transition metal and T to the surface functional group O, OH, H, or F). The dashed box indicates an approximate window of desired voltages (0.2−1.0 V) and capacities (>400 mAh/g).

dx.doi.org/10.1021/ja508154e | J. Am. Chem. Soc. 2014, 136, 16270−16276

intercalated MXenes possess highly desirable electrochemical properties. A suitable voltage for an anode material is in the range 0.2−1.0 V, which will enable a high energy density but prevent lithium plating. Ideally, the capacity should be greater than that of graphite (372 mAh/g), which is currently the dominant anode in rechargeable Li-ion batteries. This window of desirable voltages and capacities is indicated by a dashed box in Figure 3, and a number of MXenes are found in this region.

The voltages computed are for single layer MXenes, and we also investigated whether these are different for multilayer structures. Table 2 contains voltages computed for lithium intercalation into MXenes of compositions $Ti_{n+1}C_n$ and $Nb_{n+1}C_n$ (n = 1, 2, 3) with H and O functional groups. The voltages do not undergo significant changes in most cases as the number of layers in the MXene is increased. For example, in $Ti_{n+1}C_n$ the voltage is 1.22 V for a single-layer MXene, and 1.28 and 1.27 V for bilayer and trilayer structures, respectively. Although the calculated voltages in O-terminated $Nb_{n+1}C_nO_2$ are very similar, the voltage for $Nb_4C_3H_2$ is lower than those for Nb_2CH_2 and $Nb_3C_2H_2$. It is entirely possible that for multilayer MXenes the surface termination and intercalation sites will differ from those for monolayer and bilayer MXenes. A full exploration of this is required in future work. Nevertheless, the results suggest that the overall trend for monolayer MXenes is applicable to the multilayer structures.

Table 2. Cell Voltage for Lithium Intercalation into Ti- and Nb-Based Multilayer MXenes Surface Functionalized with H and O

MXene	voltage (V)	MXene	voltage (V)
Ti_2CH_2	−0.11	Nb_2CH_2	+0.19
$Ti_3C_2H_2$	−0.09	$Nb_3C_2H_2$	+0.16
$Ti_4C_3H_2$	−0.14	$Nb_4C_3H_2$	−0.02
Ti_2CO_2	+1.22	Nb_2CO_2	+0.89
$Ti_3C_2O_2$	+1.28	$Nb_3C_2O_2$	+0.79
$Ti_4C_3O_2$	+1.27	$Nb_4C_3O_2$	+0.90

To further understand the cause of the optimal electrochemical properties shown in Figure 3 and also the wide variation seen across the MXenes, we turn our attention to the effect of each individual component of the composition.

3.2. Trends in Voltage and Capacity with MXene Composition. *3.2.1. Intercalating Ion.* The most significant component in terms of the electrochemistry is the intercalating species. In Figure 3 it can be seen that there is a strong dependence of the capacity on the intercalating ion, with Mg^{2+} based compounds generally offering a higher gravimetric capacity than Li^+, Na^+, or K^+ intercalated compounds. Although Mg^{2+} has a mass about 3.5 times that of Li^+, the two-electron redox chemistry offered by each Mg^{2+} ion results in a large capacity. These data suggest that experimental efforts to intercalate Mg^{2+} into MXenes are warranted.

Besides the capacity, there is also a trend in the voltage with the intercalating species. In general, Li^+-intercalated MXenes have the highest voltages, followed in sequence by Mg^{2+}, Na^+, and K^+. Indeed, most of the K^+ compounds have a negative average voltage at the theoretical capacity indicating that intercalation of two K^+ ions per formula unit is unfavorable. This result is consistent with current experimental reports, which do not show high levels of K^+ intercalation into M_2C-based compounds.

According to eq 3, as the enthalpy change upon intercalation becomes smaller, the voltage will approach zero and can even become negative if the enthalpy change is negative. Low voltages thus indicate structures which are high in energy after intercalation. Factors that will affect the energy after intercalation are the ionic radius and ion−ion interactions of the intercalating species. Greater lateral electrostatic repulsion is expected between K^+ ions than Li^+ ions, with an increased total energy and hence lower voltage. Further support for this is found in the expansion of the in-plane lattice parameter, where the K^+ intercalated compounds undergo a larger lateral expansion than the Li^+ intercalated compounds. Other factors that influence the intercalated energies of each MXene are outlined in the next section.

3.2.2. Transition Metal Species and Surface Functional Group. To isolate the effect of the transition metal species and the surface functional groups, the data in Figure 3 are presented separately for Li^+, Na^+, and Mg^{2+} in Figure 4, where the transition metals and surface functional groups are indicated explicitly (data for K^+ are in the SI due to its low capacities). Three key results emerge.

The first feature is the variation of the capacity with the transition metal species. As expected, the MXenes containing the lighter period IV (3d) transition metals (Sc, V, Ti, Cr) offer a larger gravimetric capacity than those composed of heavier period V (4d) and VI (5d) transition metals (Zr, Nb, Mo, Hf, Ta). The range of voltages does not show a clear variation with the period of the transition metals. For example, in the lithium intercalated MXenes (Figure 4a), the transition metals of each period consistently give rise to voltages in the approximate range of −0.2 to 2.0 V. This would suggest that the d-block chemistry for each MXene is largely comparable.

A second feature, present for F- and H-functionalized and nonfunctionalized MXenes, is a correlation between the voltage and the transition metal species. As the transition metal species becomes more electropositive (e.g., Sc−Ti−V−Cr) the voltage increases. For example, Li^+ intercalation in H-functionalized compounds gives voltages of −0.30, −0.11, +0.20, and +0.35 V for Sc, Ti, V, and Cr, respectively.

The third feature is the effect of the surface functional group. For the light transition metals (Sc, Ti, V, Cr) the general picture that emerges in Figure 4 is that the voltage is typically 0.0−1.0 V for no functional groups, >0.5 V for oxygen termination, negative for H or OH termination, and a range of values for F termination. A key question then is why does a change in the functional group cause such a wide variation in the voltage for the same transition metal and intercalating species? A useful tool to illustrate the changes in the electronic structure and bonding that occur on intercalation is the charge density difference. By subtracting the charge density before intercalation from that after intercalation one can visualize any charge transfer on intercalation. Using Ti_2C as a model system, the charge density difference is shown in Figure 5 for Li intercalation in MXenes terminated with oxygen or hydrogen.

Three details are found. First, for both Ti_2CH_2 and Ti_2CO_2 there is a prominent increase in the charge density in the surface layer, which is associated with the delocalized electron density donated to the surface by Li. Second, for Ti_2CH_2 there is a slight increase in charge density between the Ti and C layers, but otherwise no significant charge transfer occurs in the central region of the 2D structure. This result suggests that the intercalation mechanism for H-termination can be considered as a simple inductive attraction between the Li^+ ion and the

dx.doi.org/10.1021/ja508154e | J. Am. Chem. Soc. 2014, 136, 16270−16276

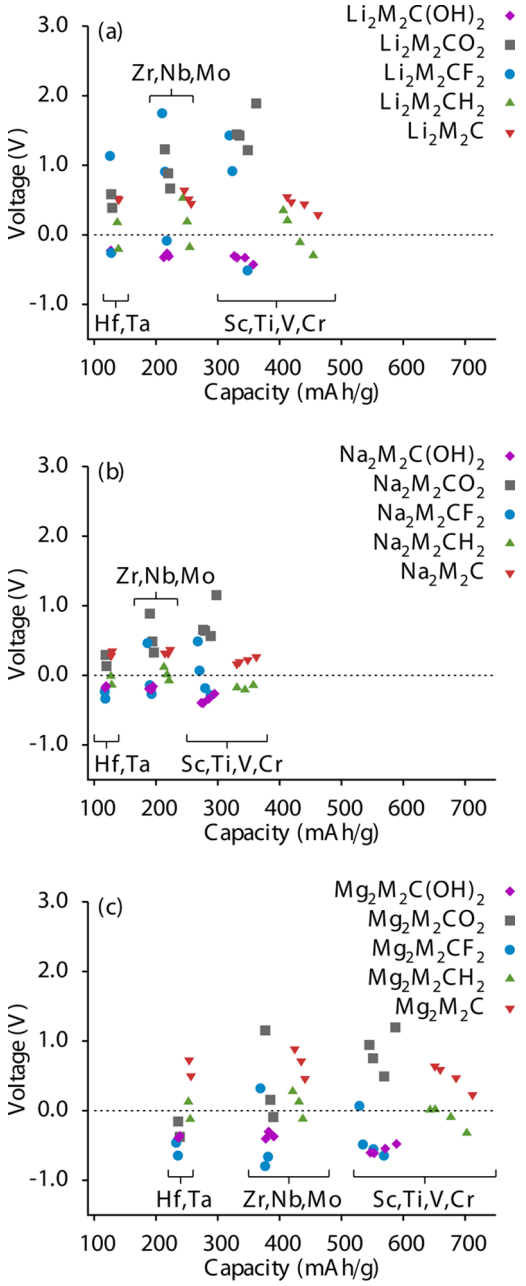

Figure 4. Cell voltage and gravimetric capacity for intercalation of two ions per formula unit into M_2C phases containing various surface functional groups: (a) Li^+ intercalation, (b) Na^+ intercalation, and (c) Mg^{2+} intercalation.

delocalized electrons it transfers onto the surface. The unfavorable voltage of −0.11 V for $Ti_2CH_2Li_2$ indicates that the surface cannot accommodate large amounts of electron density, which limits the amount of lithium that can be intercalated. Third, for Ti_2CO_2 there is extensive charge transfer around the sites within the Ti/C layer (shown in Figure 5b), suggesting a change in the Ti−O and Ti−C bond hybridization (3d-2p mixing). The higher voltage (and therefore higher energy density) for $Ti_2CO_2Li_2$ might be related to the ability to accommodate more electron density and thus a greater quantity of intercalated lithium.

This example clearly illustrates the significant changes in intercalation behavior caused by different functional groups, which will lead to a range of voltages. It is worth noting that

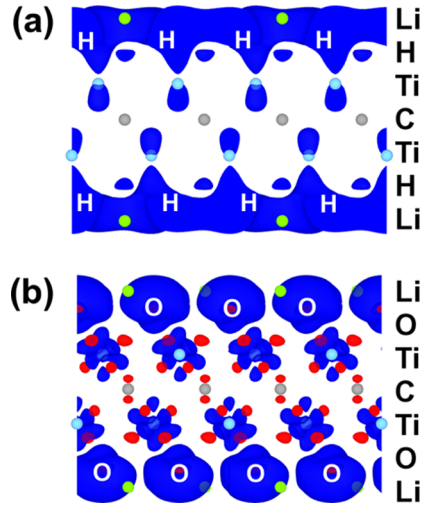

Figure 5. Charge density difference in (110) section after Li intercalaction into (a) Ti_2CH_2 and (b) Ti_2CO_2. Key: red, decrease in charge density; dark blue, increase in charge density; green, lithium; blue, titanium; gray, C. Element symbol shows positions of obscured H and O atoms. Isovalue = 0.0016.

these results are consistent with recent DFT work[17,18,51] on the electronic and surface properties of related MXenes.

As outlined earlier, the computed voltages represent an average over the theoretical capacity range. As such, compounds with average voltages close to or below zero would be expected to reach approximately half their theoretical capacity since intercalation beyond this would occur at a negative voltage. This suggests that for high-capacity MXenes, oxygen functionalization should be encouraged. The large variation in voltage and capacity with the surface functional group demonstrated here shows how alternative surface terminations would lead to MXenes with highly tunable electrochemical properties. The current synthesis method for MXenes involves treatment with HF, and it is difficult to see how O, OH, H, and F terminations can be avoided. Nevertheless, a significant improvement in the capacity might be possible if alternative synthesis routes can be found.

Finally, an intercalation mechanism has been suggested[17] based on Coulomb attraction between an induced positive charge on Li^+ and the negative functional species. Typical induced charges observed in our calculations are +0.7 for Li, +0.85 for Na, +0.4 for K, and +1.65 for Mg, and we note the two-electron process apparent in the case of the Mg ion (see SI for complete data). No clear relation between the voltage and the induced charge could be discerned. However, most MXenes are metallic, and in such materials linking delocalized electrons with particular species using techniques such as Bader analysis is problematic. Furthermore, the strong dependence, seen in Figure 4, of the voltage upon the functional group and the transition metal species suggests that the redox activity and bond rehybridization of the transition metal must also be considered in any mechanism along with the precise electronic structure. Generally, great care must be taken when attributing voltages to any single factor. It is well known, for example in polyanionic lithium battery materials,[34−38] that numerous interconnected factors can contribute toward the voltage of an electrode, including the crystal structure, redox potentials, inductive effects, and Li−Li electrostatic interactions.

dx.doi.org/10.1021/ja508154e | J. Am. Chem. Soc. 2014, 136, 16270−16276

To summarize, the most promising group of materials in terms of anode voltage (in the range 0.2−1.0 V) and gravimetric capacity (>400 mAh/g) are MXenes containing light transition metals with nonfunctionalized or O-terminated surfaces. In particular, we recommend the compositions $Li_2M_2CO_2$, Li_2M_2C (M = Sc, Ti, V, Cr) and $Mg_2M_2CO_2$, Mg_2M_2C (M = Ti, V, Cr, Nb, Mo) for attention in future work. We are aware that there are challenges in reaching the theoretical capacity of these compositions related to synthesis, processing, and electrochemistry. We stress that there are inherent difficulties in validating the calculated voltages with the few measured voltage windows and that the solid solution behavior may vary considerably between the various compounds. In unique cases, the theoretical capacities presented here may not be a precise prediction of the practical capacity. Nevertheless, our focus has been on analyzing favorable electrochemical properties by a systematic screening process to find candidate battery materials. Future computational work will address related questions on ion diffusion barriers for rate behavior, extra layers of intercalating ions and solid-solution effects.

4. CONCLUSIONS

The electrochemical properties of a large number of new 2D transition metal carbides ("MXenes") have been surveyed systematically by DFT methods. Promising materials for energy storage have been identified by examining the intercalation of Li^+, Na^+, K^+, and Mg^{2+} into M_2C-based compounds (M = Sc, Ti, V, Cr, Zr, Nb, Mo, Hf, Ta) capped with F, H, O, and OH surface functional groups. These simulations reproduce the observed trends in voltages from current experimental reports on lithiated V_2C, Ti_2C, and Nb_2C. From our global screening process, the following key results emerge:

1. A greater gravimetric capacity of Li^+ or Mg^{2+} can be intercalated into an M_2C MXene than Na^+ or K^+, which is related to the size of the intercalating ion. Compounds based on Mg^{2+} generally exhibit a higher (theoretical) gravimetric capacity than Li^+ intercalated compounds, as the two-electron redox chemistry offered by the divalent Mg^{2+} prevails over its heavier mass.
2. Variation of the surface functional group and transition metal species can significantly affect the cell voltage and gravimetric capacity of an MXene. Surface termination by oxygen tends to promote the highest capacity, whereas termination by H and/or OH should be avoided if possible since they result in a lower capacity.
3. The most promising group of materials in terms of anode voltage (in the range 0.2−1.0 V) and gravimetric capacity superior to graphite (>400 mAh/g) are M_2C compounds containing light transition metals with nonfunctionalized or O-terminated surfaces. We recognize that there are challenges in reaching the full theoretical capacity of these compositions with regard to their synthesis, processing, and electrochemistry. Overall, we recommend the compositions $Li_2M_2CO_2$, Li_2M_2C (M = Sc, Ti, V, Cr) and $Mg_2M_2CO_2$, Mg_2M_2C (M = Ti, V, Cr, Nb, Mo) for particular attention in future investigations.

In general, the results presented here provide valuable guidelines for exploring a rich variety of high-capacity M_2C-based MXenes for potential use in rechargeable batteries.

■ ASSOCIATED CONTENT

Supporting Information

Optimized structures and associated electrochemical properties of all MXene compounds considered. This material is available free of charge via the Internet at http://pubs.acs.org.

■ AUTHOR INFORMATION

Corresponding Author

m.s.islam@bath.ac.uk

Notes

The authors declare no competing financial interest.

■ ACKNOWLEDGMENTS

Financial support from the EPSRC Supergen Energy Storage Consortium (EP/H019596) and the Energy Materials Programme Grant (EP/K016288) is gratefully acknowledged. Our membership in the UK's HPC Materials Chemistry Consortium (EP/L000202) allowed use of the ARCHER computing facilities. We thank Dr. Craig Fisher (JFCC, Japan) for useful discussions.

■ REFERENCES

(1) Naguib, M.; Kurtoglu, M.; Presser, V.; Lu, J.; Niu, J.; Heon, M.; Hultman, L.; Gogotsi, Y.; Barsoum, M. W. *Adv. Mater.* **2011**, *23*, 4248−4253.

(2) Naguib, M.; Mashtalir, O.; Carle, J.; Presser, V.; Lu, J.; Hultman, L.; Gogotsi, Y.; Barsoum, M. W. *ACS Nano* **2012**, *6*, 1322−1331.

(3) Lukatskaya, M. R.; Mashtalir, O.; Ren, C. E.; Dall'Agnese, Y.; Rozier, P.; Taberna, P.-L.; Naguib, M.; Simon, P.; Barsoum, M. W.; Gogotsi, Y. *Science* **2013**, *341*, 1502−1505.

(4) Mashtalir, O.; Naguib, M.; Mochalin, V. N.; Dall'Agnese, Y.; Heon, M.; Barsoum, M. W.; Gogotsi, Y. *Nat. Commun.* **2013**, *4*, No. 1716.

(5) Naguib, M.; Come, J.; Dyatkin, B.; Presser, V.; Taberna, P.-L.; Simon, P.; Barsoum, M. W.; Gogotsi, Y. *Electrochem. Commun.* **2012**, *16*, 61−64.

(6) Yeon, S.-H.; Jung, K.-N.; Yoon, S.; Shin, K.-H.; Jin, C.-S. *J. Phys. Chem. Solids* **2013**, *74*, 1045−1055.

(7) Naguib, M.; Mochalin, V. N.; Barsoum, M. W.; Gogotsi, Y. *Adv. Mater.* **2014**, *26*, 992−1005.

(8) Khazaei, M.; Arai, M.; Sasaki, T.; Estili, M.; Sakka, Y. *Phys. Chem. Chem. Phys.* **2014**, *16*, 7841−7849.

(9) Peng, X.; Peng, L.; Wu, C.; Xie, Y. *Chem. Soc. Rev.* **2014**, *43*, 3303−3323.

(10) Hoffman, E. N.; Vinson, D. W.; Sindelar, R. L.; Tallman, D. J.; Kohse, G.; Barsoum, M. W. *Nucl. Eng. Des.* **2012**, *244*, 17−24.

(11) Khazaei, M.; Arai, M.; Sasaki, T.; Chung, C.-Y.; Venkataramanan, N. S.; Estili, M.; Sakka, Y.; Kawazoe, Y. *Adv. Funct. Mater.* **2013**, *23*, 2185−2192.

(12) Hu, Q. K.; Sun, D.; Wu, Q.; Wang, H.; Wang, L.; Liu, B.; Zhou, A.; He, J. *J. Phys. Chem. A* **2013**, *117*, 14253−14260.

(13) Gao, Q.; Zhao, X.; Xiao, Y.; Zhao, D.; Cao, M. *Nanoscale* **2014**, *6*, 6151−6157.

(14) Zhao, S. J.; Kang, W.; Xue, J. *Appl. Phys. Lett.* **2014**, *104*, No. 133106.

(15) Kurtoglu, M.; Naguib, M.; Gogotsi, Y.; Barsoum, M. W. *MRS Commun.* **2012**, *2*, 133−137.

(16) Shein, I. R.; Ivanovskii, A. L. *Comput. Mater. Sci.* **2012**, *65*, 104−114.

(17) Tang, Q.; Zhou, Z.; Shen, P. *J. Am. Chem. Soc.* **2012**, *134*, 16909−16916.

(18) Xie, Y.; Kent, P. R. C. *Phys. Rev. B* **2013**, *87*, No. 235441.

(19) Gan, L.-Y.; Huang, D.; Schwingenschlögl, U. *J. Mater. Chem. A* **2013**, *1*, 13672−13678.

(20) Enyashin, A. N.; Ivanovskii, A. L. *Comput. Theor. Chem.* **2012**, *989*, 27−32.

(21) Enyashin, A. N.; Ivanovskii, A. L. *J. Solid State Chem.* **2013**, *207*, 42−48.
(22) Enyashin, A. N.; Ivanovskii, A. L. *J. Phys. Chem. C* **2013**, *117*, 13637−13643.
(23) Wang, S.; Li, J.-X.; Du, Y.-L.; Cui, C. *Comput. Mater. Sci.* **2014**, *83*, 290−293.
(24) Tarascon, J. M.; Armand, M. *Nature* **2001**, *414*, 359−367.
(25) Whittingham, M. S. *Dalton Trans.* **2008**, 5424−5431.
(26) Ellis, B. L.; Lee, K. T.; Nazar, L. F. *Chem. Mater.* **2010**, *22*, 691−714.
(27) Goodenough, J. B.; Park, K.-S. *J. Am. Chem. Soc.* **2013**, *135*, 1167−1176.
(28) Islam, M. S.; Fisher, C. A. J. *Chem. Soc. Rev.* **2014**, *43*, 185−204.
(29) Palomares, V.; Casas-Cabanas, M.; Castillo-Martnez, E.; Han, M. H.; Rojo, T. *Energy Environ. Sci.* **2013**, *6*, 2312−2337.
(30) Dahbi, M.; Yabuuchi, N.; Kubota, K.; Tokiwa, K.; Komaba, S. *Phys. Chem. Chem. Phys.* **2014**, *16*, 15007−15028.
(31) Yoo, H. D.; Shterenberg, I.; Gofer, Y.; Gershinsky, G.; Pour, N.; Aurbach, D. *Energy Environ. Sci.* **2013**, *6*, 2265−2279.
(32) Noorden, R. V. *Nature* **2014**, *507*, 26−28.
(33) Naguib, M.; Halim, J.; Lu, J.; Cook, K. M.; Hultman, L.; Gogotsi, Y.; Barsoum, M. W. *J. Am. Chem. Soc.* **2013**, *135*, 15966−15969.
(34) Eames, C.; Armstrong, A. R.; Bruce, P. G.; Islam, M. S. *Chem. Mater.* **2012**, *24*, 2155−2161.
(35) Schroeder, M.; Eames, C.; Tompsett, D. A.; Lieser, G.; Islam, M. S. *Phys. Chem. Chem. Phys.* **2013**, *15*, 20473−20479.
(36) Clark, J. M.; Eames, C.; Reynaud, M.; Rousse, G.; Chotard, J.-N.; Tarascon, J.-M.; Islam, M. S. *J. Mater. Chem. A* **2014**, *2*, 7446−7453.
(37) Eames, C.; Clark, J. M.; Rousse, G.; Tarascon, J.-M.; Islam, M. S. *Chem. Mater.* **2014**, *26*, 3672−3678.
(38) Armstrong, A. R.; Lyness, C.; Panchmatia, P. M.; Islam, M. S.; Bruce, P. G. *Nat. Mater.* **2011**, *10*, 223−229.
(39) Armstrong, A. R.; Kuganathan, N.; Islam, M. S.; Bruce, P. G. *J. Am. Chem. Soc.* **2011**, *133*, 13031−13035.
(40) Tompsett, D. A.; Parker, S. C.; Islam, M. S. *J. Am. Chem. Soc.* **2014**, *136*, 1418−1426.
(41) Curtarolo, S.; Hart, G. L. W.; Nardelli, M. B.; Mingo, N.; Sanvito, S.; Levy, O. *Nat. Mater.* **2013**, *12*, 191−201.
(42) Mueller, T.; Hautier, G.; Jain, A.; Ceder, G. *Chem. Mater.* **2011**, *23*, 3854−3862.
(43) Jain, A.; Hautier, G.; Moore, C. J.; Ong, S.-P.; Fischer, C. C.; Mueller, T.; Persson, K. A.; Ceder, G. *Comput. Mater. Sci.* **2011**, *50*, 2295−2310.
(44) Jalem, R.; Nakayama, M.; Kasuga, T. *J. Mater. Chem. A* **2014**, *2*, 720−734.
(45) Kirklin, S.; Meredig, B.; Wolverton, C. *Adv. Energy Mater.* **2013**, *3*, 252−262.
(46) Kresse, G.; Furthmüller, J. *Phys. Rev. B. Condens. Matter* **1996**, *54*, 11169−11186.
(47) Blöchl, P. E. *Phys. Rev. B* **1994**, *50*, 17953−17979.
(48) Perdew, J. P.; Burke, K.; Ernzerhof, M. *Phys. Rev. Lett.* **1996**, *77*, 3865−3868.
(49) Shi, C.; Beidaghi, M.; Naguib, M.; Mashtalir, O.; Gogotsi, Y.; Billinge, S. J. L. *Phys. Rev. Lett.* **2014**, *112*, No. 125501.
(50) Ceder, G.; Aydinol, M. K.; Kohan, A. F. *Comput. Mater. Sci.* **1997**, *8*, 161−169.
(51) Xie, Y.; Naguib, M.; Mochalin, V. N.; Barsoum, M. W.; Gogotsi, Y.; Yu, X.; Nam, K.-W.; Yang, X.-Q.; Kolesnikov, A. I.; Kent, P. R. C. *J. Am. Chem. Soc.* **2014**, *136*, 6385−6394.